Food Chemistry 217 (2017) 469–475

Contents lists available at ScienceDirect

Food Chemistry

journal homepage: www.elsevier.com/locate/foodchem

Fluorescence spectroscopy and principal component analysis of soy protein hydrolysate fractions and the potential to assess their antioxidant capacity characteristics

Sahan A. Ranamukhaarachchi [1], Ramila H. Peiris [2], Christine Moresoli *

Department of Chemical Engineering, University of Waterloo, 200 University Avenue West, Waterloo, Ontario N2L 3G1, Canada

ARTICLE INFO

Article history:
Received 13 May 2016
Received in revised form 9 August 2016
Accepted 10 August 2016
Available online 11 August 2016

Keywords:
Soy protein hydrolysate
Antioxidant capacity
Intrinsic fluorescence
Principal component analysis
Ultrafiltration
Nanofiltration

ABSTRACT

The potential of intrinsic fluorescence and principal component analysis (PCA) to characterize the antioxidant capacity of soy protein hydrolysates (SPH) during sequential ultrafiltration (UF) and nanofiltration (NF) was evaluated. SPH was obtained by enzymatic hydrolysis of soy protein isolate. Antioxidant capacity was measured by Oxygen Radical Absorbance Capacity (ORAC) and Folin Ciocalteau Reagent (FCR) assays together with fluorescence excitation-emission matrices (EEM). PCA of the fluorescence EEMs revealed two principal components (PC_1-tryptophan, PC_2-tyrosine) that captured significant variance in the fluorescence spectra. Regression models between antioxidant capacity and PC_1 and PC_2 displayed strong linear correlations for NF fractions and a weak linear correlation for UF fractions. Clustering of UF and NF fractions according to $ORAC_{FPCA}$ and FCR_{FPCA} was observed. The ability of this method to extract information on contributions by tryptophan and tyrosine amino acid residues to the antioxidant capacity of SPH fractions was demonstrated.

1. Introduction

Antioxidant can be defined as substances that can significantly decrease the unfavorable effects of reactive species, such as oxidative free radicals, on typical human physiological functions (Halliwell & Gutteridge, 2015). Numerous well-established assays for measuring the antioxidant capacity of species are available (Apak et al., 2013). These assays can be classified as hydrogen atom transfer (HAT)- and electron transfer (ET)-assays. HAT-based assays, such as the Oxygen Radical Absorbance Capacity (ORAC), involve a complex scheme of reactions whereby an antioxidant and a substrate compete for peroxy radicals that are thermally generated by the breakdown of azo-compounds (Apak, Özyürek, Güçlü, & Çapanoğlu, 2016). In the ORAC assay, the antioxidant capacity of a specie is deduced from the fluorescence decay curve and the associated area under the curve (AUC) reflecting its oxidative degradation by peroxy radicals (Apak et al., 2007). ET assays, such as the Folin Ciocalteau's reducing capacity (FCR) and ferric reducing antioxidant power (FRAP) assays, involve a redox-potential probe (i.e., fluorescent or colored probe). Antioxidant capacity is thus measured by the reduction of an oxidant with a single electron transfer upon which a color change in solution can be observed and spectrophotometrically quantified (Apak et al., 2007). ET mechanisms employ non-physiological conditions (i.e., room temperature, pH conditions that are not representative of human physiology) to measure the reducing capacity of a molecule in the absence of reactive free radicals, whereas ORAC combines relative inhibition and time for inhibition of free radicals into one quantity to provide a superior indication of antioxidant capacity of a specie than ET mechanisms (Preedy, 2011; Cao & Prior, 1998).

Many proteins, such as soy proteins, can contain correct amino acid and peptide sequences for bioactive functions. However, these peptides are restricted from performing these functions within the sequence of their native protein by peptide bonds, which occupy the terminal ends of an amino acid's backbone structure (amino- and carboxyl-termini), and by side chain interactions between peptide chains. Upon liberation from their native protein sequence, certain peptides can fulfill antioxidant functions among other bioactive properties (Chen, Muramoto, Yamauchi, Fujimoto, & Nokihara, 1998). A number of amino acid residues, including histidine, tyrosine, tryptophan, phenylalanine, proline, and leucine, have been identified as contributors to antioxidant

* Corresponding author.
E-mail address: cmoresol@uwaterloo.ca (C. Moresoli).
[1] Presently at the Department of Electrical and Computer Engineering, University of British Columbia, Vancouver, BC V6T 1Z4, Canada.
[2] Presently at Sanofi Pasteur Canada, 1755 Steeles Avenue West, Toronto, ON M2R 3T4, Canada.

http://dx.doi.org/10.1016/j.foodchem.2016.08.029
0308-8146/

Nomenclature

AAPH	2,2′-Azobis-2-methyl-propanimidamide dihydrochloride
AUC	Area under the curve
EEM	Excitation-emission matrix
ET	Electron transfer
Ex/Em	Excitation and emission wavelengths
FCR	Folin Ciocalteau Reagent assay
FCR_{FPCA}	Fluorescence- and PCA-estimated FCR
FRAP	Ferric reducing antioxidant power
HAT	Hydrogen atom transfer
MLRM	Multi-linear regression model
MWCO	Molecular weight cut off (kDa)
NF	Nanofiltration
OPA	O'phthaldialdehyde
ORAC	Oxygen Radical Absorbance Capacity assay
$ORAC_{FPCA}$	Fluorescence- and PCA-estimated ORAC
PC	Principal component
PCA	Principal component analysis
PMMA	Polymethylmethacrylate
PMT	Photomultiplier tube
RS	Rayleigh light scattering
SPH	Soy protein hydrolysate
SPI	Soy protein isolate
SSE	Sum of squared errors
TE	Trolox equivalents
TMP	Transmembrane pressure (Pa, N m^{-2})
TS	Total solid content (g L^{-1})
UF	Ultrafiltration

capacity in peptides (Hartmann & Meisel, 2007; Nimalaratne, Lopes-Lutz, Schieber, & Wu, 2011). One of the highly antioxidant peptides identified in soy protein hydrolysates is leucine-leucine-proline-histidine-histidine peptide (leu-leu-pro-his-his) (Chen et al., 1998). The his-his portion of this leu-leu-pro-his-his peptide was the primary contributor to its antioxidative property. It was found that pro-his-his, as an individual peptide, displayed the highest antioxidant capacity. Furthermore, the presence of a leucine or proline residue at the amino-terminus of a his-his-containing peptide enhanced the antioxidant capacity and hydrophobicity of the peptides (Hartmann & Meisel, 2007). Histidine and other aromatic amino acids contribute to antioxidant capacity, due to their ring structures (Nimalaratne et al., 2011). However, the antioxidant capacity of a histidine residue is greater within a peptide, compared to when it stands alone, due to synergistic effects with other amino acid residues, like those from proline and leucine.

ORAC antioxidant capacity assay is a time consuming method with multiple steps and prolonged analysis times. FCR assay is relatively less time consuming compared to the ORAC assay, but requires multiple steps during preparation and to obtain measurements for analysis (Margraf, Karnopp, Rosso, & Granato, 2015). Given the importance of these assays and the challenges faced with their use, novel and rapid methods to capture relative antioxidant capacities of samples are of interest in food, nutrition and medicine.

Intrinsic fluorescence refers to fluorescence caused by a chemical compound, known as a fluorophore, which can re-emit light at a higher wavelength upon excitation at a lower wavelength (Zhang, Müller, Wu, & Feld, 2000). Intrinsic fluorescence spectroscopy, a non-destructive analytical tool, presents many advantages and applications in biological processes; it is rapid, has high sensitivity, specificity, and reproducibility. Many naturally occurring fluorophores are present in the cellular environment including tyrosine, tryptophan, phenylalanine, retinol, and riboflavin (Christensen, Nørgaard, Bro, & Engelsen, 2006; Teixeira, Duarte, Carrondo, & Alves, 2011). Fluorescence analysis has been used to investigate protein structures (based on the intrinsic fluorescence of aromatic amino acids) (Bron, Ribeiro, Azzolini, Jacomino, & Machado, 2004; Christensen et al., 2006). At a given excitation wavelength (Ex), fluorescence intensities of a sample can be collected at a range of emission wavelengths (Em) to construct a fluorescence landscape, known as an excitation-emission matrix (EEM). The analysis of these EEMs is challenging due to the high volume of data points and the high degree of co-linearity present between intensity data captured at different excitation and emission wavelength combinations.

Multivariate statistical methods, such as principal component analysis (PCA), can be used for extracting specific and sensitive information from the fluorescence EEM intensity data. PCA is often used to capture variances and extract significant systematic trends in sample data sets that contain large amounts of variables (Christensen et al., 2006; Oliveira, Calado, Ares, & Granato, 2015; Peiris, Budman, Moresoli, & Legge, 2009; Zielinski et al., 2014). PCA can be used to observe the correlations between fluorescence signals and important bioprocess variables (Teixeira et al., 2011). A detailed description of PCA can be found in Eriksson, Johansson, Kettaneh-Wold, and Wold (2001).

The objectives of this work were to investigate the tryptophan and tyrosine content of soy protein hydrolysate fractions produced during sequential UF and NF membrane operations by intrinsic fluorescence spectroscopy and PCA, and evaluate potential correlations with the ORAC and FCR antioxidant capacity of these fractions.

2. Materials and methods

2.1. Materials

Soy protein isolate (SPI) PRO-FAM 974 powder was obtained from Archer Daniels Midland Company, Decatur, IL, USA. Pepsin from porcine stomach mucosa, pancreatin mixture from porcine pancreas, 99.9% sodium borate decahydrate (S9640-500G), sodium dodecyl sulfate (L4509-250G), phthaldialdehyde (P0657-5G), FCR reagent (F9252), 2,2′-azobis-2-methyl-propanimidamide dihydrochloride (AAPH, 440914-25G), and Trolox (6-hydroxy-2,5,7,8-tetramethylchroman-2-carboxylic acid; 238813-1G) were obtained from Sigma-Aldrich, St. Louis, MO, USA. *L*-(+)-α-phenyl-glycine (2935-35-5) from MP Biomedical, Solon, OH, USA; Fluorescein (065-00252) from Wako Pure Chemical Industries, Osaka, Japan; and sodium carbonate (SX0400-1 500G) from EMD Chemicals, Gibbstown, NJ, USA. Hollow fibre polysulfone UF membrane module (UFP-10-E-4MA; 10 kDa MWCO, active area of 4.2×10^{-2} m^2) was purchased from Amersham Biosciences, Westborough, MA, USA. A G10 thin film composite NF membrane (2.5 kDa MWCO, active area of 1.4×10^{-2} m^2) was purchased from Sterlitech Corporation, Kent, WA, USA.

2.2. Preparation of soy protein hydrolysates

SPI was dissolved in MilliQ water to obtain a 3.12% (w/v) solution. The SPI solution was either subjected to heat treatment (95 °C during 5 min) or subjected to enzymatic hydrolysis as described

previously (Ranamukhaarachchi, Meissner, & Moresoli, 2013). Briefly summarized, hydrolysis was performed with 0.5% (w/v) pepsin at 37 °C and pH 1.5 for 30 min, followed by hydrolysis with 0.5% (w/v) pancreatin mixture at 40 °C and pH 7.8 for 60 min. Heat treatment and enzymatic hydrolysis were performed in 500 mL batches, until 2000 mL of soy protein hydrolysate were collected. SPH were frozen at −20 °C until use.

2.3. Filtration experiments

Ultrafiltration (UF) and nanofiltration (NF) experiments were performed as described previously (Ranamukhaarachchi et al., 2013). Briefly summarized, UF was conducted with a hollow fibre polysulfone UF membrane module at 62 kPa transmembrane pressure (TMP), 2.4 L min^{-1} feed flow rate, and room temperature (22 °C). The feed volume was 1100 mL, and the filtration was stopped when 650 mL of permeate was collected. Frozen SPH samples were thawed overnight, and ultracentrifuged (Sorvall WX Ultra 100; Thermo Scientific, Asheville, NC, USA) with a A-621 rotor (31,901 G and 22 °C during 30 min) to remove non-dissolved solids. UF retentate and permeate fractions were sampled at the end of filtration and frozen at −20 °C. Feed, retentate and permeate fractions were evaluated for total solids (TS) content, ORAC and FCR antioxidant capacities, and analyzed via fluorescence spectroscopy.

The UF permeate fractions were subsequently fractionated by NF. NF experiments were conducted in a cross-flow SEPA CF II cell (GE Osmonics, Minnetonka, MN, USA) with G10 thin film composite NF membrane. A feed volumetric flow rate of 1.8 L min^{-1}, a TMP of 2.0 MPa and a temperature of 22 °C were selected. NF was conducted until 50% of feed volume was collected in the permeate stream (volume concentration ratio = 2).

The feed solution was prepared with thawed UF permeate fractions and diluting with MilliQ water to a TS of 1.0 g L^{-1} and a final feed volume of 2.0 L. Ten NF experiments were performed overall: (i) four NF for SPH (no SPI heat treatment) at pH 4 and 8, (ii) six NF for SPH (with SPI heat treatment, H-SPH) at pH 4 and 8. Two of the NF experiments for H-SPH (at pH 4 and 8) were sampled for permeate and retentate fractions at 5 min. intervals during filtration generating 96 NF permeate and retentate samples. During the eight remaining NF experiments for the SPH and H-SPH, permeate and retentate fractions were sampled at the end of filtration and frozen at −20 °C. All NF fractions were evaluated for TS, ORAC and FCR antioxidant capacities, and analyzed using fluorescence spectroscopy.

2.4. Analytical methods

2.4.1. Total solids (TS) determination

A known volume of a sample was placed on an aluminum dish (VWR, Mississauga, ON, Canada), and incubated overnight in a conventional oven at 105 °C to evaporate the moisture. Dry mass in the dish was determined, which provided a direct measure of TS content of the sample.

2.4.2. O'phthaldialdehyde (OPA) assay

OPA spectrophotometric assay was used for total peptide determination (estimated by equivalent phenyl-glycine concentration) as described previously (Ranamukhaarachchi et al., 2013). The OPA calibration curve consisted of a phenyl-glycine concentration range from 0 to 1.0 mmol L^{-1}. Triplicate measurements were conducted per sample hydrolysate fraction.

2.4.3. Oxygen Radical Absorbance Capacity (ORAC) assay

The ORAC method was adapted from Cao, Alessio, and Cutler (1993) as described previously (Ranamukhaarachchi et al., 2013). An ORAC calibration curve was prepared for a Trolox concentration range of 0–100 μM. A black 96-well plate was used to analyze all samples and standard solutions. A volume of 100 μL of a 2.5 nM Fluorescein solution was added to each well followed by 50 μL of sample or standard solution. The plate was covered with a plastic 96-well plate lid and incubated at 37 °C for 15 min, prior to the addition of 50 μL of AAPH solution to each well. A Synergy 4 microplate reader (BioTek, Winooski, VT, USA) was used for the analysis of Fluorescein degradation. A temperature of 37 °C was maintained with constant shaking to optimize peroxy radical formation by AAPH. Fluorescence Ex/Em was 485/520 nm. Fluorescence measurements were collected every minute for 120 min. The antioxidant capacity was determined by measuring the area under the fluorescence decay plots generated with and without the antioxidant, known as the area under the curve (AUC). Antioxidant capacity was expressed as concentration of Trolox equivalents (TE) per total solids content. Triplicate ORAC measurements were conducted per sample hydrolysate fraction.

2.4.4. Folin Ciocalteau's reducing capacity (FCR) assay

The FCR method was adapted from Folin and Ciocalteu (1927) as described previously (Ranamukhaarachchi et al., 2013). Briefly summarized, an FCR calibration curve was prepared using a Trolox concentration range of 0–3 mM. Volumes of 20 μL of sample or trolox standard were added to 4.5 mL polymethylmethacrylate cuvettes (PMMA; UV-grade; VWR, Mississauga, ON, Canada). Each cuvette was incubated for 5 min at 22 °C after adding 150 μL of FCR reagent. Then, 600 μL of 15% (w/v) sodium carbonate was added to each cuvette followed by 2230 μL of MilliQ water to achieve a final volume of 3 mL. The cuvettes were shaken and incubated for 120 min at room temperature (22 °C). UV absorbance measurements at 750 nm were obtained using the Spectronic Genesys 2 spectrophotometer (Milton Roy, Ivyland, PA, USA). Triplicate FCR measurements were conducted per sample hydrolysate fraction.

2.5. Fluorescence analysis

Fluorescence analyses were performed according to Peiris et al. (2009) and Peiris, Hallé, et al. (2010) with the following modifications: the emission spectra were obtained at a photomultiplier tube (PMT) voltage of 650 V, medium scanning rate, an excitation slit width of 5 nm, and an emission slit width of 5 nm. A fluorescence EEM for a sample was generated by scanning Ex from 250 to 340 nm and Em from 300 to 600 nm, thereby producing 4214 Ex/Em data points per EEM.

2.5.1. Principal component analysis

The methodology for principal component analysis (PCA) was performed according to Peiris, Budman, Moresoli, and Legge (2010). Permeate and retentate fractions collected at 5 min. intervals from the two NF experiments with H-SPH at pH 4 and 8 produced 96 samples for the "NF data set". These 96 samples were divided in two data matrices; one data matrix contained 47 fluorescence EEMs representing NF samples for H-SPH at pH 4 (matrix X_{NF4}) and it was used in the PCA calibration step. This PCA calibration is referred to as PCA_{NF} hereforth, as it only involved the NF samples. The second data matrix contained 49 EEMs representing NF samples for H-SPH at pH 8 (matrix X_{NF8}), and it was used to validate the PCA_{NF} model. Validation of the PCA model was necessary to ensure that the developed model was accurate for other independent data. The selection of X_{NF4} and X_{NF8} data matrices for PCA calibration and validation were made randomly, and can be performed in reverse, as well. Both X_{NF4} and X_{NF8} data sets were subjected to auto-scaling by subtracting each intensity reading by the mean of each column wavelength intensity, and dividing by the standard deviation.

A second PCA calibration (referred to as PCA_{UF}) was developed with the EEMs of 8 UF samples (matrix Z_{UF} consisting of both SPH and H-SPH samples) to demonstrate the potential of this method described herein to evaluate biological samples other than dilute, nanofiltered substances. The UF samples contained highly concentrated, larger peptides fractions compared to NF fractions. The PCA_{UF} model developed with UF samples was validated with the EEMs of 112 NF fractions (matrix Z_{NF}), which included the 96 fractions from X_{NF4} and X_{NF8}, and 16 additional NF permeate and retentate fractions from the remaining eight NF experiments with SPH and H-SPH (described in Section 2.3). The combined data set of Z_{UF} and Z_{NF} contained 120 samples and was termed "UF-NF data set".

2.6. Multi-linear regression analysis of principal components

Separate PCA analyses performed on the X_{NF} and X_{UF} data resulted in two statistically significant PCs each for X_{NF} and X_{UF} data sets that captured the maximum variance present in the fluorescence EEM data. These PCs were therefore used in the development of the MLRMs according to Elshereef (2009). Two MLRMs were developed by correlating the PCs with the measured ORAC for NF (PCA_{NF}) and UF-NF (PCA_{UF}) data sets in the format of Eq. (1). Similarly, another two MLRMs were developed by correlating the PCs with the measured FCR for NF (PCA_{NF}) and UF-NF (PCA_{UF}) data sets in the format of Eq. (2). The purpose of building the MRLMs for the UF-NF data set was to validate this approach for larger molecular weight peptide fractions, as described below in Section 3.3.

$$ORAC_{FPCA} = \beta_0 + \beta_1 \cdot PC_1 + \beta_2 \cdot PC_2 \quad (1)$$

$$FCR_{FPCA} = \alpha_0 + \alpha_1 \cdot PC_1 + \alpha_2 \cdot PC_2 \quad (2)$$

Fluorescence and PCA estimated ORAC is referred to as $ORAC_{FPCA}$, and fluorescence and PCA estimated FCR is referred to as FCR_{FPCA}. The β_0, β_1, and β_2 terms refer to the parameters estimated by minimizing the sum of squared error (SSE) between $ORAC_{FPCA}$ and measured ORAC values. The terms β_1 and β_2 can be considered as the individual contribution of the fluorescence components of PC_1 and PC_2 to ORAC. Similarly, α_0, α_1 and α_2 parameters were estimated by minimizing the SSE between FCR_{FPCA} and measured FCR values. Also, the terms α_1 and α_2 can be considered as the individual contribution of the fluorescence components of PC_1 and PC_2 to FCR.

From the NF data set (n = 96; H-SPH), all NF permeate samples at pH 4 and 8 (n = 47) were used to build the MLRM equations for ORAC and FCR. The remaining NF retentate samples (n = 49) were used to validate the MLRMs. From the UF-NF data set (n = 120; used in PCA_{UF}), 60 samples were randomly selected (mixture of both UF and NF samples) to develop the MLRMs for ORAC and FCR antioxidant capacity. The remaining 60 samples were used for validation of the MLRM equations. Adjusted R^2 values were determined for plots of MLRMs, as a measure of goodness-of-fit of linear regression (Steel, Dickey, & David, 1997). The normality assumptions were assessed using residual analysis with the Shapiro-Wilk test (Shapiro & Wilk, 1965).

3. Results and discussion

3.1. Fluorescence EEMs for UF and NF peptide fractions

Soy protein hydrolysate fractions with different peptide content, total solids content, and antioxidant capacity were obtained by sequential UF and NF operations at pH 4 and 8. Typical fluorescence EEMs for UF and NF permeate fractions at pH 4 and 8 (Fig. 1) contain two regions representing amino acid-containing substances (peak α and shoulder δ) and a region corresponding to Rayleigh light scattering (RS). Fluorescence regions identified by α and δ represent tryptophan and tyrosine, respectively (Baker, 2002; Christensen et al., 2006). Tryptophan fluoresces at Ex/Em ~275 nm/350 nm, and tyrosine at Ex/Em ~275 nm/305 nm (Baker, 2002). The region corresponding to RS was previously related to colloidal substances in water (Peiris, Budman, et al., 2010).

3.2. Effects of UF and NF on peptide distribution and antioxidant capacity

UF fractions possessed significantly higher peptide concentrations (1.52–3.65 mmol L^{-1}) and TS content (17.66–30.43 g L^{-1}) than NF fractions (0.026–0.295 mmol L^{-1} and 0.10–2.20 g L^{-1}, respectively).

The measured ORAC and FCR antioxidant capacity of the UF and NF (pH 4 and 8 combined) samples collected during membrane filtration steps are presented in Fig. 2. Due to the fundamental differences between the two antioxidant assays employed in this study, there was no considerable correlation between measured ORAC and FCR for both UF ($R^2 = 0.09$) and NF ($R^2 = 0.30$) fractions (Fig. 2a). The ORAC and FCR antioxidant capacity of all peptide fractions collected during the sequential UF and NF are provided in *Supplement Material* section.

Upon separating the NF samples based on their separation pH conditions, weak correlations were found between the measured ORAC and FCR ($R^2 = 0.63$ at pH 4 and $R^2 = 0.66$ at pH 8), shown in Fig. 3a. However, these correlations do not indicate a considerable difference to infer any influence of pH on the relationship between measured ORAC and FCR antioxidant capacity of UF peptide fractions. The correlation between the $ORAC_{FPCA}$ and FCR_{FPCA} presented in Figs. 2b and 3b are discussed in detail later in Section 3.4.

The ranges of measured ORAC values for UF and NF samples were 903–3068 and 860–5562 μmol TE g^{-1}, respectively. Similarly, the ranges of measured FCR values for UF and NF samples were 182–321 and 187–1678 μmol TE g^{-1}, respectively.

3.3. PCA of fluorescence profiles for NF peptide fractions

PCA of the fluorescence intensity for the NF fractions obtained at pH 4 (PCA_{NF} of X_{NF4} matrix; n = 47) generated five statistically significant PCs, which captured 72.8% of the total variance in these NF fractions. PC_1 (25%) and PC_2 (18.5%) represented 43.5% of variance, while PC_3, PC_4, and PC_5 cumulatively captured 29.3% of variance. The remaining 27.2% of variance not captured by these five PCs was assumed to be due to instrument noise in fluorescence readings (~5%) and other unknown sources.

The loading values associated with each PC were arranged according to the corresponding Ex/Em wavelength combinations in the data matrix, which generated a loading matrix (Peiris, Hallé, et al., 2010). By investigating this loading matrix in terms of their respective fluorescence Ex/Em wavelength coordinates, spectral features of each PC may be identified (Persson & Wedborg, 2001). The loading plot for PC_1 (Fig. 4a) displayed a predominant peak (α′) at Ex/Em ~280 nm/400 nm, which was similar to the region where tryptophan (α peak in Fig. 1) appeared; therefore, PC_1 scores serve as surrogate measurements of the tryptophan content in the fractions. Similarly, PC_2 (a dominant valley (δ′) at Ex/Em ~275 nm/310 nm; Fig. 4b) serve as surrogate measurements of the tyrosine content in the fractions, where PC_2 scores would be inversely related to the tyrosine content of the fractions. Since these two statistically significant PCs were associated with amino acids residues known to contribute to antioxidant capacity, PC_1 and PC_2 scores were used to develop indicators of

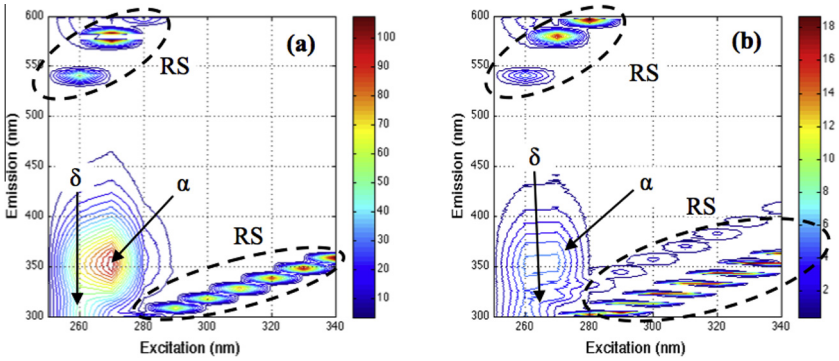

Fig. 1. Fluorescence features observed in typical fluorescence EEM for (a) UF permeate (peptide content of 0.076 mmol g^{-1}; TS of 20.2 g L^{-1}) and (b) NF permeate at pH 8 (peptide content of 0.125 mmol g^{-1}; TS of 0.4 g L^{-1}) for soy protein hydrolysate with heat treatment. Fluorescence regions identified by α and δ represent tryptophan and tyrosine amino acids, respectively. Rayleigh light scattering (RS) regions are indicated by the dashed lines.

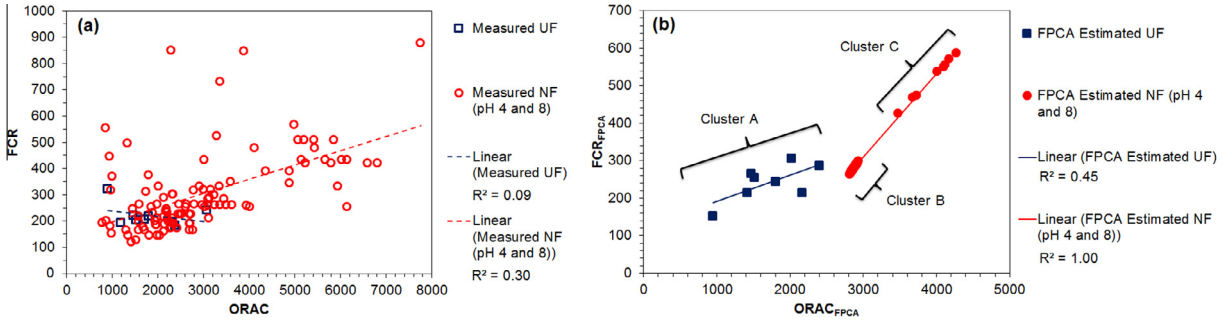

Fig. 2. Measured FCR against measured ORAC antioxidant capacity for UF (n = 8) and NF (n = 112) soy protein hydrolysate samples with and without heat treatment (a); and fluorescence and PCA estimated FCR (FCR_{FPCA}) against ORAC ($ORAC_{FPCA}$) antioxidant capacity for UF (n = 8) and NF (n = 112) soy protein hydrolysate samples with and without heat treatment (b).

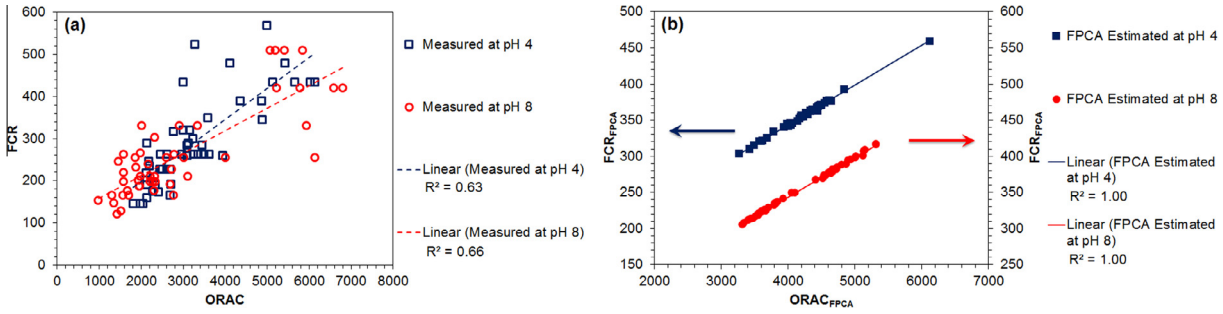

Fig. 3. Measured FCR against measured ORAC antioxidant capacity for NF soy protein hydrolysate samples with and without heat treatment at pH 4 (n = 47) and pH 8 (n = 49) (a); and fluorescence and PCA estimated FCR (FCR_{FPCA}) against ORAC ($ORAC_{FPCA}$) antioxidant capacity for NF soy protein hydrolysate samples with and without heat treatment at pH 4 (n = 47) and pH 8 (n = 49) (b).

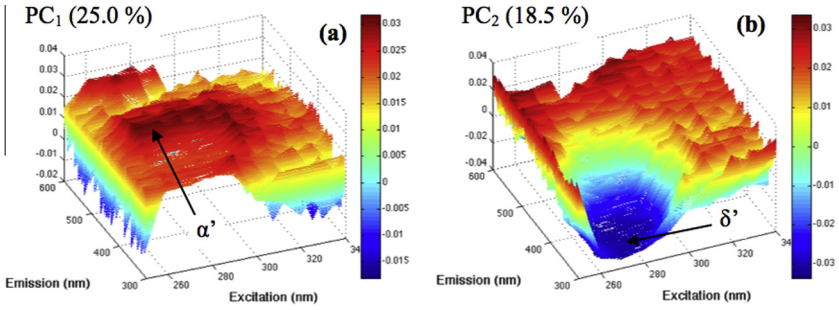

Fig. 4. Three-dimensional representation of the loading matrices obtained by PCA of NF fluorescence data (X_{NF4}) for (a) PC_1 and (b) PC_2. Variance captured by each PC is provided in brackets.

$ORAC_{FPCA}$ and FCR_{FPCA} antioxidant capacity of the NF fractions, with MLRMs, as described in Section 2.6. The other significant PCs (PC_3, PC_4, and PC_5) were not associated with amino acids based on the loading plots.

Since only NF fractions were used to estimate $ORAC_{FPCA}$ and FCR_{FPCA} antioxidant capacities from PCA_{NF}, verification was necessary to determine if this relationship would hold true for larger molecular weight soy protein hydrolysate fractions. Therefore, PCA_{UF} was conducted with the UF-NF data set, and MLRMs were developed, as described in Section 2.6. Two statistically significant PCs were identified from PCA_{UF}, capturing a total variance of 89.4% (55.2% by PC_1 and 34.2% by PC_2). Based on the PC loading plots (results not shown; results are similar to the loading plots presented in Fig. 4) and fluorescence features, PC_1 was related to the tryptophan content and PC_2 was related to the tyrosine content.

3.4. Fluorescence and PCA-captured relative ORAC and FCR antioxidant capacities during fractionation of SPH

Strong linear correlations ($R^2 > 0.99$, adjusted $R^2 > 0.99$) between estimated FCR (FCR_{FPCA}) and ORAC ($ORAC_{FPCA}$) antioxidant capacities (Eqs. (1) and (2) in Section 2.6) were observed for the NF fractions at pH 4 and 8 (Fig. 3b). Normality assumptions for the MLRMs described in Section 2.6 were confirmed through residual analysis. This linear relationship suggested that the tryptophan and tyrosine content of the NF fractions deduced from their fluorescence characteristics was directly related to the antioxidant capacity captured in the ORAC and FCR analysis, which agreed with previously published work that also showed the influence of tryptophan and tyrosine on antioxidant capacity of peptides (Huang, Ou, & Prior, 2005; Nimalaratne et al., 2011). The pH conditions employed during NF did not appear to affect the estimated $ORAC_{FPCA}$ and FCR_{FPCA} antioxidant capacity (Fig. 3b), indicating that the combined contribution of tryptophan and tyrosine-containing peptide fractions to ORAC and FCR antioxidant capacity was pH and charge independent.

The FCR assay is known to give a direct measure of the total phenolic content (chemical compounds with a hydroxyl group bonded to an aromatic hydrocarbon group), which for peptides is due predominantly to the presence of aromatic amino acids (i.e., tyrosine and tryptophan) (Huang et al., 2005). The role of tyrosine and tryptophan as key contributors in the ORAC antioxidant capacity of peptides from egg yolk was shown previously by Nimalaratne et al. (2011). This contribution was not directly evident when correlating the measured ORAC to the measured FCR for NF and UF samples (Fig. 2a), as there may have been other molecules present in the peptide fractions that contributed to measured ORAC and FCR antioxidant capacity that did not fluoresce. In addition, the fundamental differences in the underlying antioxidant mechanisms of the ORAC and FCR assays may also have contributed to these weak correlations (Apak et al., 2007; Cao & Prior, 1998; Huang et al., 2005). Previous studies have indicated that FCR and ORAC methods should be considered simultaneously to reflect the complexity of antioxidant capacity (Frankel & Meyer, 2000; Huang et al., 2005). In this context, our proposed fluorescence EEM and PCA approach have provided the common properties relevant to antioxidant capacities from ORAC and FCR measurements. The biological features in peptides that influence both ORAC and FCR antioxidant capacity have been detected, identified and assessed through this proposed method. It can be viewed as a method for extracting the information related to the contribution of tryptophan and tyrosine peptide fractions to the antioxidant capacity of ORAC and FCR measurements.

During the PCA_{UF}, which was conducted to explore the potential of the proposed method to assess more concentrated peptide fractions, a weak linear relationship for the UF samples ($R^2 = 0.45$, adjusted $R^2 = 0.23$; n = 8), and a significantly improved linear relationship for the NF samples ($R^2 > 0.99$, adjusted $R^2 > 0.99$; n = 112) were observed between the estimated ORAC and FCR values (Fig. 2b) confirming observations for NF samples at pH 4 and 8 in Fig. 3b. The weak fit of the antioxidant capacity of UF samples could be attributed to the limited number of samples employed in this study (n = 8); and/or their variations with respect to heat treatment prior to enzymatic hydrolysis, peptide concentrations (1.52–3.65 mmol L^{-1}), and TS content (17.66–30.43 g L^{-1}). The magnitude of the variations for the peptide concentrations (0.026–0.295 mmol L^{-1}) and TS contents (0.10–2.20 g L^{-1}) of NF samples was extremely low compared to UF samples. The differences in the separation mechanisms between UF and NF could also explain this limited fit for UF data. Since the molecular weight of the UF fractions was significantly larger compared to the NF fractions, their antioxidant capacity was found to be lower as a result of the confinement of antioxidative amino acid residues by peptide bonds and side chain interactions (Ranamukhaarachchi et al., 2013). Meanwhile, their fluorescence intensity may have increased with molecular weight due to the presence of a higher concentration of fluorophores (Christensen et al., 2006; Park, Lee, Baek, & Lee, 2010). The broader molecular weight distribution on antioxidant capacity and fluorescence emission intensity may have contributed to a larger variation in UF samples compared to NF samples consequently influencing their $ORAC_{FPCA}$ and FCR_{FPCA} values, and the limited fit (Fig. 2b).

A clustering effect of the UF (cluster A) and NF (cluster C) samples from SPH was observed according to the estimated FCR_{FPCA} antioxidant capacity upon closer observation in Fig. 2b. The NF fractions produced from H-SPH (cluster B) had similar estimated FCR_{FPCA} antioxidant capacity to UF fractions (cluster A), but displayed distinct $ORAC_{FPCA}$ values. The NF fractions produced two clusters (clusters B and C) along both estimated $ORAC_{FPCA}$ and FCR_{FPCA} axes (Fig. 2b), distinguishing each other based on heat treatment of SPI prior to enzymatic hydrolysis. The NF fractions from SPH resulted in higher $ORAC_{FPCA}$ and FCR_{FPCA} (cluster C) antioxidant capacity compared to H-SPH (cluster B).

Plots of observed versus fluorescence and PCA estimated ORAC and FCR antioxidant capacity were used to examine the contributions of other non-fluorescing amino acids to the ORAC and FCR measurements, but were not captured by the fluorescence EEM and PCA method. A plot of observed ORAC versus $ORAC_{FPCA}$ values provided a moderate linear fit for UF samples ($R^2 = 0.66$, adjusted $R^2 = 0.52$; data not shown), and no linear fit for NF samples. Observed FCR vs. FCR_{FPCA} values showed a weak relationship for UF and NF samples (data not shown). Therefore, the proposed method helps identify common features/contributors that impact antioxidant capacity, and provides information to help improve the understanding of and disparity between the used antioxidant assays/mechanisms.

3.5. Potential of fluorescence features of peptide fractions

In this study, PCA of fluorescence EEMs for UF and NF soy protein hydrolysate fractions combined with multi-linear regression analysis of the principal components allowed for the examination of the underlying relationship between the ORAC and FCR antioxidant capacity assays with distinct mechanisms. This method related fluorescence features assigned to tryptophan and tyrosine to the antioxidant capacity of soy protein hydrolysate fractions. Thus, this approach represents a potential avenue to assess tryptophan and tyrosine features captured by ORAC and FCR antioxidant assays. The proposed method has potential applications in food and nutraceutical screening and quality control processes, where multiple biological components that impact the antioxidant capacity in a sample can be identified, quantified, and evaluated along

with their bioactive functionalities in one simple, rapid measurement.

4. Conclusion

Principal component analysis (PCA) of fluorescence excitation-emission matrix data for UF and NF soy protein hydrolysate (SPH) fractions, followed by multi-linear regression analysis captured tryptophan and tyrosine features and FCR and ORAC antioxidant capacity characteristics. Two statistically significant principal components (PC_1 and PC_2) were related to the tryptophan and tyrosine content of the SPH fractions. Estimation of the ORAC ($ORAC_{FPCA}$) and FCR (FCR_{FPCA}) antioxidant capacity based on principal components developed from intrinsic fluorescence of NF fractions showed strong linear relationships ($R^2 > 0.99$, adjusted $R^2 > 0.99$). The following key conclusions were made:

1. Linear relationship was observed between the estimated $ORAC_{FPCA}$ and FCR_{FPCA} for NF fractions indicating that the tryptophan and tyrosine content of these fractions are major contributors to the antioxidant capacity captured in the ORAC and FCR assays.
2. The pH condition during NF did not affect the relationship between estimated ORAC and FCR antioxidant capacity.
3. Weak linear relationship observed between the estimated $ORAC_{FPCA}$ and FCR_{FPCA} of the UF samples was attributed to the limited number of samples ($n = 8$), and the large molecular weight of these fractions.
4. A clustering effect distinguished the estimated $ORAC_{FPCA}$ of the UF from NF soy protein hydrolysate fractions irrespective of SPI heat treatment.
5. A clustering effect distinguished the estimated $ORAC_{FPCA}$ and FCR_{FPCA} of the NF soy protein hydrolysate fractions in terms of SPI heat treatment.

Hence, the proposed approach represents a promising avenue to assess fundamental features of protein hydrolysates with antioxidant capacity.

Conflict of interest

The authors have no conflicts of interest to declare.

Acknowledgement

The authors wish to acknowledge the Natural Sciences and Engineering Research Council of Canada (NSERC) for the financial support.

Appendix A. Supplementary data

Supplementary data associated with this article can be found, in the online version, at http://dx.doi.org/10.1016/j.foodchem.2016.08.029.

References

Apak, R., Güçlü, K., Demirata, B., Özyürek, M., Çelik, S. E., Bektaşoğlu, B., Berker, K. I., & Özyurt, D. (2007). Comparative evaluation of various total antioxidant capacity assays applied to phenolic compounds with the CUPRAC assay. *Molecules, 12*(7), 1496–1547.

Apak, R., Gorinstein, S., Böhm, V., Schaich, K. M., Özyürek, M., & Güçlü, K. (2013). Methods of measurement and evaluation of natural antioxidant capacity/activity (IUPAC Technical Report). *Pure and Applied Chemistry, 85*(5), 957–998.

Apak, R., Özyürek, M., Güçlü, K., & Çapanoğlu, E. (2016). Antioxidant activity/capacity measurement. 2. Hydrogen atom transfer (HAT)-based, mixed-mode (electron transfer (ET)/HAT), and lipid peroxidation assays. *Journal of Agricultural and Food Chemistry, 64*(5), 1028–1045.

Baker, A. (2002). Fluorescence properties of some farm wastes: implications for water quality monitoring. *Water Research, 36*(1), 189–195.

Bron, I. U., Ribeiro, R. V., Azzolini, M., Jacomino, A. P., & Machado, E. C. (2004). Chlorophyll fluorescence as a tool to evaluate the ripening of 'Golden' papaya fruit. *Postharvest Biology and Technology, 33*(2), 163–173.

Cao, G., Alessio, H. M., & Cutler, R. G. (1993). Oxygen-radical absorbance capacity assay for antioxidants. *Free Radical Biology and Medicine, 14*(3), 303–311.

Cao, G., & Prior, R. L. (1998). Comparison of different analytical methods for assessing total antioxidant capacity of human serum. *Clinical Chemistry, 44*(6), 1309–1315.

Chen, H.-M., Muramoto, K., Yamauchi, F., Fujimoto, K., & Nokihara, K. (1998). Antioxidative properties of histidine-containing peptides designed from peptide fragments found in the digests of a soybean protein. *Journal of Agricultural and Food Chemistry, 46*(1), 49–53.

Christensen, J., Nørgaard, L., Bro, R., & Engelsen, S. B. (2006). Multivariate autofluorescence of intact food systems. *Chemical Reviews, 106*(6), 1979–1994.

Elshereef, R. (2009). *Application of multi-wavelength fluorometry to monitoring protein ultrafiltration*, Thesis 60. University of Waterloo.

Eriksson, L., Johansson, E., Kettaneh-Wold, N., & Wold, S. (2001). *Multi-and megavariate data analysis, principles and applications*. 91-973730-1-X. Umea, Sweden: Umetrics Academy.

Folin, O., & Ciocalteu, V. (1927). On tyrosine and tryptophane determinations in proteins. *Journal of Biological Chemistry, 73*(2), 627–650.

Frankel, E. N., & Meyer, A. S. (2000). The problems of using one-dimensional methods to evaluate multifunctional food and biological antioxidants. *Journal of the Science of Food and Agriculture, 80*(13), 1925–1941.

Halliwell, B., & Gutteridge, J. M. (2015). *Free radicals in biology and medicine*. USA: Oxford University Press.

Hartmann, R., & Meisel, H. (2007). Food-derived peptides with biological activity: from research to food applications. *Current Opinion in Biotechnology, 18*(2), 163–169.

Huang, D., Ou, B., & Prior, R. L. (2005). The chemistry behind antioxidant capacity assays. *Journal of Agricultural and Food Chemistry, 53*(6), 1841–1856.

Margraf, T., Karnopp, A. R., Rosso, N. D., & Granato, D. (2015). Comparison between Folin-Ciocalteu and Prussian blue assays to estimate the total phenolic content of juices and teas using 96-well microplates. *Journal of Food Science, 80*(11), C2397–C2403.

Nimalaratne, C., Lopes-Lutz, D., Schieber, A., & Wu, J. (2011). Free aromatic amino acids in egg yolk show antioxidant properties. *Food Chemistry, 129*(1), 155–161.

Oliveira, C. C. D., Calado, V. M. D. A., Ares, G., & Granato, D. (2015). Statistical approaches to assess the association between phenolic compounds and the in vitro antioxidant activity of Camellia sinensis and Ilex paraguariensis teas. *Critical Reviews in Food Science and Nutrition, 55*(10), 1456–1473.

Park, S. Y., Lee, J. S., Baek, H. H., & Lee, H. G. (2010). Purification and characterization of antioxidant peptides from soy protein hydrolysate. *Journal of Food Biochemistry, 34*(s1), 120–132.

Peiris, B., Budman, H., Moresoli, C., & Legge, R. (2009). Acquiring reproducible fluorescence spectra of dissolved organic matter at very low concentrations. *Water Science and Technology, 60*(6).

Peiris, R. H., Budman, H., Moresoli, C., & Legge, R. L. (2010). Understanding fouling behaviour of ultrafiltration membrane processes and natural water using principal component analysis of fluorescence excitation-emission matrices. *Journal of Membrane Science, 357*(1), 62–72.

Peiris, R. H., Hallé, C., Budman, H., Moresoli, C., Peldszus, S., Huck, P. M., & Legge, R. L. (2010). Identifying fouling events in a membrane-based drinking water treatment process using principal component analysis of fluorescence excitation-emission matrices. *Water Research, 44*(1), 185–194.

Persson, T., & Wedborg, M. (2001). Multivariate evaluation of the fluorescence of aquatic organic matter. *Analytica Chimica Acta, 434*(2), 179–192.

Preedy, V. R. (2011). *Beer in health and disease prevention*. Academic Press.

Ranamukhaarachchi, S., Meissner, L., & Moresoli, C. (2013). Production of antioxidant soy protein hydrolysates by sequential ultrafiltration and nanofiltration. *Journal of Membrane Science, 429*, 81–87.

Shapiro, S. S., & Wilk, M. B. (1965). An analysis of variance test for normality (complete samples). *Biometrika, 52*(3/4), 591–611.

Steel, R. G., Dickey, J. H., & David (1997). *Principles and procedures of statistics a biometrical approach*. WCB/McGraw-Hill.

Teixeira, A. P., Duarte, T. M., Carrondo, M., & Alves, P. M. (2011). Synchronous fluorescence spectroscopy as a novel tool to enable PAT applications in bioprocesses. *Biotechnology and Bioengineering, 108*(8), 1852–1861.

Zhang, Q., Müller, M. G., Wu, J., & Feld, M. S. (2000). Turbidity-free fluorescence spectroscopy of biological tissue. *Optics Letters, 25*(19), 1451–1453.

Zielinski, A. A., Haminiuk, C. W., Nunes, C. A., Schnitzler, E., Ruth, S. M., & Granato, D. (2014). Chemical composition, sensory properties, provenance, and bioactivity of fruit juices as assessed by chemometrics: a critical review and guideline. *Comprehensive Reviews in Food Science and Food Safety, 13*(3), 300–316.